



1 **Molecular fingerprinting of particulate organic matter as a new tool** 2 **for its source apportionment: changes along a headwater drainage in** 3 **coarse, medium and fine particles as a function of rainfalls**

4 Laurent Jeanneau^{1*}; Richard Rowland²; Shreeram Inamdar²

5 ¹ OSUR, UMR 6118 Géosciences Rennes, Université de Rennes 1 – CNRS, Rennes, France

6 ² Water Science & Policy Graduate Program, University of Delaware, Newark, USA

7 *Correspondence to:* Laurent Jeanneau (laurent.jeanneau@univ-rennes1.fr)

8 **Abstract.** Tracking the sources of particulate organic matter (POM) exported from catchments is important to understand the
9 transfer of energy from soils to oceans. The suitability of investigating the molecular composition of POM by thermally
10 assisted hydrolysis and methylation using tetramethylammonium hydroxide directly coupled to gas chromatography and
11 mass spectrometry is presented. The results of this molecular fingerprint approach were compared with previously published
12 elemental (%C, %N) and isotopic data ($\delta^{13}\text{C}$, $\delta^{15}\text{N}$) acquired in a nested headwater catchment in Piedmont region, Eastern
13 United States of America (12 and 79 ha). The concordance between these results highlights this molecular tool as a valuable
14 method for source fingerprinting of POM. It emphasizes litter as the main source of exported POM at the upstream location
15 ($80 \pm 14\%$) with an increasing proportion of stream bed (SBed) sediments remobilization downstream ($42 \pm 29\%$),
16 specifically during events characterized by high rainfall amounts. At the upstream location, the source of POM seems to be
17 controlled by the maximum and median hourly rainfall intensity. An added-value of this method is to directly investigate
18 chemical biomarkers and to mine their distributions in term of biogeochemical functioning of an ecosystem. In this
19 catchment, the distribution of plant-derived biomarkers characterizing lignin, cutin, and suberin inputs were similar in SBed
20 and litter, while the proportion of microbial markers was 4 times higher in SBed than in litter. These results indicate that
21 SBed OM was largely from plant litter that has been processed by the aquatic microbial community.



22 1 Introduction

23 Particulate organic matter (POM) plays key-roles in aquatic ecosystems, controlling the transfer and the bioavailability of
24 energy, nutrients and micropollutants. The flux of POM from soils to oceans has been estimated at 0.2 GtC per year (Ludwig
25 et al., 1996) with 80 % coming from biospheric inputs and the complement from petrogenic inputs (Galy et al., 2015).
26 Assuming that the energy provided by natural organic matter is equivalent of the energy provided by the combustion of
27 wood, this flux of POM corresponds to an energy of 2.8 EJ, that is to say less than 2 days of the global energy consumption
28 of 2015 (yearbook.enerdata.net). This export mainly occurs during storm events, those hot moments being responsible for up
29 to 80% of annual particulate organic carbon (POC) export depending on the investigated catchment (Dhillon and Inamdar,
30 2013; Jeong et al., 2012; Jung et al., 2012; Oeurng et al., 2011).

31 Among these hot moments, extreme events, defined as storm flow exceeded less than 10 % of the time (IPCC, 2001), seem
32 to play a dominant role. In two contrasted catchments, a mountainous one in South-Korea and a lowland one in the Eastern
33 United States of America (USA), the specific POC flux (flux per unit area of the catchment) has been shown to be non
34 linearly related to total rainfall with a threshold value beyond which the slope increased sharply (Dhillon and Inamdar, 2013;
35 Jung et al., 2014). The threshold value (approx. 70 mm in the American catchment and approx. 120 mm in the South-Korean
36 catchment) and the magnitude of this increase differed between both catchments and are probably watershed-dependant. Is
37 the non linearity of the relationship between rainfall amount and POC export observed previously linked to a modification of
38 the source of POM? POM in a river system is a combination of allochthonous and autochthonous OM. The former is derived
39 mainly from the soils and banks erosion, while the latter can be composed of fresh aquatic living organisms and bed
40 sediments. The balance between these different sources is controlled (i) by the catchment' size and morphology and (ii) by
41 the rainfall event characteristics (Tank et al., 2010).

42 Tracking the sources of POM can be done indirectly by investigating the sources of suspended matter. This can be done
43 through the analysis of fallout radionuclides such as Beryllium-7, Lead-210 and Cesium-137 (Ritchie et al., 1974; Wallbrink
44 and Murray, 1996; Walling, 1998) or by geochemical fingerprinting of rare elements (Collins and Walling, 2002). It can also
45 be done directly by investigating the composition of POM using bulk-scale descriptors such as OC and Nitrogen
46 concentrations, C/N ratio and stable isotopes $\delta^{13}\text{C}$ and $\delta^{15}\text{N}$ (Fox and Papanicolaou, 2008). Molecular biomarkers analyses
47 have also been used. They are based on specific molecular classes such as lipid or lignin biomarkers (Goñi et al., 2013; Jung
48 et al., 2015). Thermochemiolysis using tetramethylammonium hydroxide coupled to gas chromatography and mass
49 spectrometry has already been applied to the investigation of the fate of river DOM (Jeanneau et al., 2015) and POM
50 (Mannino and Harvey, 2000). This analytical technique is widely used to investigate the biogeochemistry of soil organic
51 matter (Derenne and Quéneá, 2015) and, coupled to a principal component analysis (PCA), it has been shown to be valuable
52 for forensic soils applications (Lee et al., 2012). An advantage of such an analysis is to generate a distribution of more than
53 hundred identified target compounds with small amount of particulate matter (from 5 to 10 mg) (Jeanneau et al., 2014),
54 giving a dataset rich enough to differentiate between sources (Walling, 2013). Here this analytical approach is combined



55 with a principal component analysis (PCA) to determine the main sources of POM as a function of the sediment size, the
56 catchment size and the rainfall characteristics.

57 The first objective of this paper is to test the suitability of molecular biomarkers derived from THM-GC-MS as a tool to
58 determine the sources of river POM. The second objective is to investigate how the sources of POM changed as a function of
59 the catchment size, particle size of the sediment, and the hydrological characteristics of the rainfall events. This study is
60 based on a subset of samples used to investigate the sources of POM exported during storm events using ^{13}C and ^{15}N as
61 tracers (Rowland et al., 2017). We hypothesized that molecular biomarkers provide important insights into sources of POM
62 and can be used as complimentary tracers for POM alongside or in addition to stable isotopes.

63 2 Material and methods

64 2.1 Site description

65 This study was conducted in a 79 ha watershed (second order stream) located in the Piedmont physiographic region of
66 Maryland, USA (Figure 1). The watershed drains into the Big Elk Creek which discharges into the Chesapeake Bay. For a
67 detailed description of the study site, refer to Rowland et al. (2017). Briefly, the watershed is predominantly forested with
68 pasture along the outer periphery. Dominant canopy species include *Fagus grandifolia* (American beech), *Liriodendron*
69 *tulipifera* (yellow poplar), and *Acer rubrum* (red maple). Bedrock formations consist of metamorphic gneiss and schist and
70 soils are coarse loamy, mixed, mesic lithic inceptisols on slopes and oxyaquic inceptisols in saturated valley bottoms.
71 Elevations in the watershed range from 77 to 108 m with slope gradients ranging from 0.16 to 24.5° (mean 6.3°). Mean
72 annual precipitation from 1981 to 2010 in this region was 1173.5 mm, with late spring and late summer as the wettest and
73 driest periods, respectively, and mean annual temperature is 13°C (Delaware State Climatologist Office Data Page, 2016).

74 2.2 Watershed monitoring and sampling strategy

75 Detailed information on monitoring and sampling is provided in Rowland et al. (2017). Climatological data was obtained
76 from a local station maintained by the Delaware Environmental Observing System approximately 450 m from the 79 ha
77 catchment outlet. This consists of temperature and GEONOR gage hourly rainfall measurements. Stream discharge estimates
78 were obtained at 20-minute intervals using a Parshall flume at 12 ha stream location (nested within the 79 ha watershed,
79 Figure 1) and a discharge rating curve calculated from paired pressure transducer and acoustic Doppler velocity meter
80 measurements at a rectangular concrete culvert at the 79 ha location.

81 Suspended sediments were collected using in-situ samplers made of 10 cm diameter capped PVC pipes placed vertically in
82 the middle of the stream. The upstream face of the pipes was perforated with 1.5 cm diameter holes beginning ~10 cm above
83 the stream bed. During periods of elevated discharge, stream stage rose above the perforations, trapping suspended sediment
84 within the sampler. The trapped sediment thus represented a time-integrated composite sediment sample (CSS). All CSS
85 were retrieved within 24 hours of the end of an event and frozen prior to processing and analysis.



86 Seven potential sediment sources were identified within the catchment and have been sampled at three locations to integrate
87 their spatial heterogeneity (Rowland et al., 2017). These included the stream bed (SBed), exposed stream bank A (BaA) and
88 B (BaB) horizons, valley-bottom wetland surficial soils (W), forest floor litter (Li) and humus (FH) and the upland A
89 horizons (Up). Sampling was conducted during the summer of 2015. 500-750 g of each end-member were sampled using an
90 ethanol-cleaned trowel or auger from both of the main tributary branches of the watershed. Stream beds were sampled from
91 areas without major backwatering or pooling, as POM may undergo diagenesis here, and were composited along a three by
92 three-point grid within the channel. Bank sediments were collected from exposed incised banks with three points composited
93 from the A and B horizons. Forest floor litter and humus, valley-bottom wetland soils and upland A horizons samples were
94 composited from five points along 20 m transects in low gradient locations in order to integrate their spatial heterogeneity.
95 End-member soil and sediment samples and CSS were dried in acid-cleaned Pyrex dishes in an oven at 45°C until visibly
96 dry. Oven-dry CSS samples were partitioned into coarse (CPOM) > 1000 µm, medium (MPOM) 1000-250 µm and fine
97 (FPOM) < 250 µm size classes via dry sieving. Dry masses were recorded for particle size class from which the fractional
98 mass percent was calculated for each class in each CSS sample. End-member samples were pre-sieved at 2 mm to remove
99 large organic debris such as roots. Aliquots were lyophilized overnight and preserved in a desiccator cabinet until elemental,
100 isotopic and molecular analyses. CSS and end-member samples were pulverized and homogenized using a ceramic mortar
101 and pestle that was cleaned with ethanol between samples.

102 2.3 Analytical methodology

103 For elemental and isotopic analyses, please refer to Rowland et al., (2017). The thermochemolysis using
104 tetramethylammonium hydroxide (TMAH) coupled to gas chromatography and mass spectrometry (THM-GC-MS) was
105 performed according to Jeanneau et al. (2014). Briefly we introduced approximately 5 mg of freeze-dried solid residue into
106 an 80 µL aluminum reactor with an excess of solid TMAH (ca. 10 mg) and 10 µl of a solution of dihydrocinnamic acid d9
107 (CDN Isotopes, ref. D5666) diluted at 25 µg/ml in methanol as an internal standard. The THM reaction was performed on-
108 line using a vertical micro-furnace pyrolyser PZ-2020D (Frontier Laboratories, Japan) operating at 400°C. The products of
109 this reaction were injected into a gas chromatograph (GC) GC-2010 (Shimadzu, Japan) equipped with a SLB 5MS capillary
110 column in the split mode (60 m × 0.25 mm ID, 0.25 µm film thickness). The temperature of the transfer line was 321°C and
111 the temperature of the injection port was 310°C. The oven was programmed to maintain an initial temperature of 50°C for 2
112 minutes, then rise to 150°C at 15°C min⁻¹, and then rise to 310°C at 3 °C min⁻¹ where it stayed for 14 minutes. Helium was
113 used as the carrier gas, with a flow rate of 1.0 ml/min. Compounds were detected using a QP2010+ mass spectrometer (MS)
114 (Shimadzu, Japan) operating in the full scan mode. The temperature of the transfer line was set at 280°C, the ionization
115 source at 200°C, and molecules were ionized by electron impact using an energy of 70 eV. The list of analyzed compounds
116 and m/z ratios used for their integration are given in the supplementary materials (Table S1). Compounds were identified on
117 the basis of their full-scan mass spectra by comparison with the NIST library and with published data (Nierop et al., 2005;



118 Nierop and Verstraten, 2004). They were quantified assuming similar ionization and detection efficiencies between all
119 compounds. This assumption means that the concentrations must be handled as rough estimations.

120 Target compounds were classified into four categories: low molecular weight organic acids (LOA), phenolic compounds
121 (PHE) including lignin and tannin markers, carbohydrates (CAR) and fatty acids (FA). The peak area of the selected m/z
122 (mass/charge) for each compound was integrated and corrected by a mass spectra factor (MSF) calculated as the reciprocal
123 of the proportion of the fragment used for the integration and the entire fragmentogram provided by the NIST library (Table
124 S1). The proportion of each compound class was calculated by dividing the sum of the areas of the compounds in this class
125 by the sum of the peak areas of all analyzed compounds expressed as a percentage. The analytical uncertainty for this
126 analytical method, expressed as a relative standard deviation ranged from 10 to 20% depending on the samples and the target
127 compounds. The use of THM-GC-MS to investigate the sources of POM meant that it was necessary to assume that matrix
128 effects are equivalent for all analyzed compounds in all samples.

129 **2.4 Statistical analyses and calculation of the proportions of the main sources of POM in CSS**

130 Statistical analyses were performed using XLSTAT (version 19.01, Addinsoft). First a principal component analysis (PCA)
131 was performed using the end-members as individuals and CSS as additional individuals. The relative proportions of the 112
132 target compounds and the sum of their concentrations in ng/mg of freeze-dried matrix were used as variables. The relative
133 distribution of target compounds allows the direct comparison of the different samples without concentration effect, while
134 using the sum of their concentrations takes into consideration the fact that the concentration of target compounds differed
135 from a sample to another.

136 The first PCA allows identifying the correlated variables on the basis of a modulus of the Pearson coefficient > 0.9 . When
137 two variables were correlated, the least abundant was removed. Then a second PCA was performed. The variables with a
138 correlation lower than 0.4 with the two first factors (F1: 29.8%; F2: 17.2% of variance) were removed, resulting in a new set
139 of 71 variables. A third PCA was calculated and a hierarchical ascendant classification (HAC) was calculated using the
140 coordinates of the individuals (end-members and CSS) on the 9 first factors that explained 90.5% of the variance of the
141 dataset. This HAC identified Upland soils and Stream bank sediments as minor contributors. Consequently a fourth PCA
142 was calculated removing Upland soils and Stream bank sediments from the potential end-members. Similarly to the three
143 previous PCA, CSS were considered as additional individuals. The coordinates of CSS on the two first factors (on 10) of this
144 PCA (F1: 40.1%; F2: 24.0% of variance) were used to calculate the proportion of the three main sources of POM in CSS
145 identified as 1. stream bed sediments, 2. litter and 3. forest floor humus + wetland soil, resolving a system of equations with
146 three unknowns. To solve this system, the coordinates of end-members must be specified. The heterogeneity of the
147 distribution of target compounds resulted in an area for each end-member. To calculate the proportions and uncertainties, the
148 coordinates of end-members were randomly selected ten times in the areas defined by the 95% IC. When the calculation
149 gave a negative contribution for an end-member, it was set at 0 and the two others contributions were recalculated to sum at
150 100. Finally the contributions of those three sources were approximated for the bulk POM by using the proportion and the



151 OC content of each fraction. From the third PCA to the end of the procedure, this treatment was also performed adding TOC,
152 $\delta^{13}\text{C}$ and $\delta^{15}\text{N}$ from Rowland et al. (2017) as variables.
153 In order to test the efficiency of the source apportionment calculated with the molecular data, the proportions of end
154 members and their isotopic values (Rowland et al., 2017) were used to model the $\delta^{13}\text{C}$ of CSS. Modeled values were
155 compared to measured values reported by Rowland et al. (2017) by calculating the relative standard deviation (RSD) and
156 against a linear regression model.

157 3 Results

158 3.1 Rainfall and hydrology

159 The molecular composition of POM in coarse, medium and fine size classes was investigated for four events. The rainfall
160 and discharge characteristics recorded for those events are indicated in Table 1. The total rainfall ranged from 40.1 (E4) to
161 148.9 (E1) mm, the maximum hourly rainfall (I_{max}) ranged from 19.9 (E1) to 31.3 (E3) mm h^{-1} and the median hourly
162 rainfall (I_{med}) ranged from 0.4 (E3) to 2.2 (E2) mm h^{-1} . The maximum discharge for those events ranged from 15.6 (E4) to
163 150.1 (E1) l s^{-1} . Then the four events can be distinguished as follows. E1 was characterized by high rainfall, a low maximum
164 intensity (I_{max}), a mean median intensity (I_{med}) and a mean antecedent precipitation index (API7). E2 was characterized by
165 mean total rainfall, a mean I_{max} , a high I_{med} and a mean API. E3 was characterized by high rainfall and I_{max} , low I_{med}
166 and high API7. Finally E4 was characterized by low rainfall and I_{max} , a high I_{med} and a dry antecedent conditions (API7 =
167 0 mm). E2 and E4 were comparable in terms of precipitation regime but can be differentiated by the API7, E4 occurring
168 after 7 days without precipitation.

169 3.2 Size distribution

170 CSS were separated into coarse (>1 mm), medium (>250 μm) and fine (<250 μm) fractions, with the exception of CSS at the
171 downstream (79 ha) location for the fourth event (Table 1). In the 12 ha sub-catchment, the coarse, medium and fine
172 fractions represented 22 ± 20 , 22 ± 4 and 55 ± 21 % of particulate matter, respectively, while in the 79 ha catchment, they
173 represented 61 ± 19 , 22 ± 10 and 18 ± 10 % of particulate matter, respectively. In the 12 ha sub-catchment, the relative
174 standard deviation (RSD) of those proportions was 90, 17 and 37 % for the coarse, medium and fine fractions, respectively,
175 while in the 79 ha catchment it was 31, 45 and 55 %, respectively.

176 3.3 Molecular composition of end-members

177 The number of detected target compounds ranged from 49 (SBed#1) to 112 (FH). A Dixon test for extreme value identified
178 the lowest value (SBed#1) as an outlier (p -value = 0.011). Once this value removed, the number of detected target



179 compounds ranged from 75 (BaB) to 112 (FH). The low value recorded for one of the SBed could be due to a combination of
180 a low OC content with a low analytical efficiency. This sample was removed from the dataset.

181 The distribution of target compounds into chemical families gives a first overview of the molecular composition of OM in
182 the different end-members (Figure 2). In W, Li and FH, the main compounds are PHE and high molecular weight FA ($> C_{20}$,
183 HMW) that represent more than 30% of target compounds. In BaA and BaB, the proportion of PHE was lower (22 ± 4 and
184 19 ± 1 %, respectively; mean \pm SD) than in W, Li and FH and the proportion of LMW FA was higher (27 ± 17 and 35 ± 9 %,
185 respectively). In Up, compared to W, Li and FH, the proportion of HMW FA increased (57 ± 19 %), while the proportion of
186 PHE decreased (13 ± 8 %). In SBed, the main identified target compounds were LMW FA (72 ± 8 %), while PHE and HMW
187 FA represented 15 ± 2 % and 9 ± 4 %, respectively.

188 HMW FA was composed of linear *n*-alkanoic acids from *n*- $C_{20:0}$ to *n*- $C_{32:0}$ with an even-over-odd predominance
189 characteristic of plant-derived inputs (Eglinton and Hamilton, 1967), linear ω -hydroxyacids and α,ω -diacids from *n*- C_{16} to *n*-
190 C_{28} , 10,16-dihydroxy $C_{16:0}$ and 9,10,18-trihydroxy $C_{18:0}$ characteristic of plant-derived aliphatic biopolymers cutin and suberin
191 (Armas-Herrera et al., 2016; Kolattukudy, 2001). These two latter hydroxyacids were the main compounds among HMW
192 FA. The proportion of ω -hydroxyacids and α,ω -diacids among HMW FA is higher in roots than in leaves and can be used to
193 differentiate between suberin from roots and cutin from shoots (Mueller et al., 2012). This proportion decreased from soils
194 (Up, FH and W) and bank sediments to litter and was minimal for SBed (17 ± 8 %), highlighting that the proportion of cutin
195 decreased from SBed, Li to bank sediments and soils.

196 PHE was composed of methoxy-benzene, -acetophenone, -benzaldehyde and -benzoic acids. These compounds derived from
197 lignin and tannins and are characteristic of plant-derived OM. The main compounds were guaiacyl-like structures: 3,4-
198 dimethoxybenzaldehyde, 3,4-dimethoxybenzoic acid methyl ester, *erythro* and *threo*-1,2-dimethoxy-4-(1,2,3-
199 trimethoxypropyl)benzene and syringil-like structures: 3,4,5-trimethoxybenzaldehyde and 3,4,5-trimethoxybenzoic acid
200 methyl ester, which is typical of the THM-GC-MS of OM deriving from woody plants (Challinor, 1995). Benzoic acid was
201 not classified in PHE since it was negatively (slope of the linear regression model: -0.20; -0.18; -0.17) and poorly correlated
202 (Pearson coefficient, *p*-value: 0.14, 0.002; 0.14, 0.002; 0.21, <0.001) with 3,4-dimethoxybenzoic acid methyl ester, 3,4,5-
203 trimethoxybenzoic acid methyl ester and 3-(3,4-dimethoxyphenyl)prop-2-enoic acid methyl ester, respectively, that are the
204 main representatives of the three types of lignin units analyzed by THM-GC-MS (Challinor, 1995). As a consequence, it was
205 not considered to calculate the proportion of molecules coming from lignins and tannins.

206 LMW FA included *n*-alkanoic acids from *n*- $C_{6:0}$ to *n*- $C_{19:0}$, *iso* and *anteiso* $C_{13:0}$, $C_{15:0}$ and $C_{17:0}$, *iso* $C_{14:0}$ and $C_{16:0}$ and *n*-
207 alkenoic acids *n*- $C_{16:1}$ and *n*- $C_{18:1}$. The LMW FA with less than 13 C atoms can derive from microbial or plant-derived
208 inputs, while the LMW FA with more than 13 C atoms are known as phospholipid fatty acids (PLFA) and are microbial
209 biomarkers (Frostegård et al., 1993). The proportion of microbial markers among target compounds was calculated
210 according to Jeanneau et al. (2014). It increased from litter and soils (<15%) to bank sediments (18 ± 12 % and 25 ± 7 % in
211 BaA and BaB, respectively) to SBed (48 ± 15 %).



212 3.4 Molecular composition of stream suspended sediments

213 The distribution of target compounds into the five chemical families previously described changed with the catchment size
214 as illustrated on Figure 3. At the 12 ha location, this distribution was fairly homogenous across the particle classes. When
215 averaged across size fractions and events, the THM-GC-MS of the POM of CSS sampled at the 12 ha location mainly
216 produced PHE (48 ± 6 %, mean \pm SD) and HMW FA (22 ± 10 %). The relative standard deviation weighted by the
217 proportion (RSDp) was 13, 14 and 22 % for C, M and F fractions, respectively, which highlights a low inter-event variability
218 of this distribution. At the 79 ha location, the distribution of target compounds was dominated by LMW FA (41 ± 20 %) and
219 PHE (37 ± 9 %). It was almost stable between the three size fractions with a higher proportion of LMW FA in the M
220 fraction. However, the RSDp was 50, 55 and 23 % for C, M and F fractions, respectively, which means a higher inter-event
221 variability than at the 12 ha location.

222 3.5 End-members contributions

223 A hierarchical ascendant classification (HAC) was performed using the coordinates of end-members and stream sediments
224 (CSS) on the nine first factors (90.5 % of variance) of the PCA, which were calculated with the relative proportions of target
225 compounds and the sum of their concentrations as variables. Three classes were isolated. The first one included the three Li,
226 one FH and one W as end-members, the size fractions of CSS from the 12 ha location and 3 size fractions of CSS from the
227 79 ha location. The second group included two W, two FH and the three BaA, BaB and U end-members. Finally the third
228 group included the SBed end-members and the size fractions of CSS from the 79 ha location. Based on this HAC, U, BaA
229 and BaB were considered as minor contributors to the POM exported from the 12 ha and 79 ha locations.

230 An additional PCA was then calculated using SBed, Li, FH and W as individuals, CSS as additional individuals, and the
231 previously defined list of 71 variables. The two first factors of this PCA explained 64.1 % of the variance of this final
232 dataset. The projection of end-members and CSS on the plan obtained with these two factors is illustrated on Figure 4. This
233 projection allows differentiating: (i) the three groups of end-members, Li, SBed and a combination of FH and W, denoted
234 FH-W and (ii) POM from the two sampling locations. Moreover the size classes were also separated. From this 2D
235 projection, an area was defined for each end-member corresponding to the 95% CI. The results of the source apportionment
236 calculated using this 2D projection are listed in Table 2.

237 At the 12ha location, as an average of the four sampled events, from FPOM to CPOM, the proportion of OM coming from
238 SBed decreased from 17 ± 16 % (mean \pm SD) to 1 ± 1 %, the proportion of OM coming from FH-W decreased from 16 ± 16
239 % to 8 ± 12 % and the proportion of OM coming from Li increased from 67 ± 7 % to 90 ± 11 %. The large uncertainties
240 quantified by the mean RSD (78 ± 53 %, mean \pm SD, $n = 9$) reflected the inter-storm variability of this source
241 apportionment. Bulk POM was mainly inherited from Li with contributions ranging from 65 to 92 %.

242 At the 79ha location, as an average of the four sampled events, CPOM was mainly inherited from Li (63 ± 28 %) and SBed
243 (36 ± 30 %). MPOM was mainly due to SBed inputs (49 ± 39 %) and received a substantial contribution of FH-W (17 ± 31



244 %) . Similarly to CPOM, FPOM was mainly inherited from Li (55 ± 15 %) and SBed (38 ± 24 %). Similarly to the source
245 apportionment at the 12ha location, the large uncertainties ($RSD = 97 \pm 57$ %, $n = 9$) were due to inter-storm variability.
246 Bulk POM was mainly inherited from Li with contributions ranging from 42 to 89 % and SBed with contributions ranging
247 from 8 to 57 %.

248 4 Discussions

249 4.1 What are the main sources of POM for the watershed?

250 The HAC identified four main end-members for the stream water POM: litter (Li), the surface horizon of forest soils (FH)
251 and wetland soils (W) and stream bed sediments (SBed). Li was the main source of POM identified along the catchment
252 representing 80 ± 14 % and 49 ± 24 % of the POM exported from the 12 ha and 79 ha catchments, respectively. These high
253 proportions of Li-derived POM is in accordance with the results of Jung et al. (2015) where isotopic and *n*-alkanes
254 fingerprints of POM exported from a mountainous forested headwater catchment highlighted similarities with litter and
255 surface soils. Moreover the decrease in the proportion of Li-derived OM along the catchment fits well with the observation
256 of Koiter et al. (2013) where the contribution of topsoil sources of suspended sediments decreased from 75 to 30 % when
257 moving downstream.

258 Stream bank A and B horizons and the surface horizons of upland soils did not group with any CSS, which would mean that
259 they were minor contributors for the investigated samples. This seems to be in contradiction with the documented impact of
260 bank erosion on the mobilization of particulate organic matter (Adams et al., 2015; Nosrati et al., 2011; Tamooh et al.,
261 2012). This apparent contradiction could be due to the catchment's size. Contrary to the previously cited investigations
262 (Adams et al., 2015; Nosrati et al., 2011; Tamooh et al., 2012), this present study focused on a headwater catchment (0.79
263 km²). In these small catchments, POM mainly comes from the erosion of surrounding soils as observed for monsoon floods
264 in Laos (Gourdin et al., 2015; Huon et al., 2017) or from a combination of bedrock and surface erosion in an Alpine
265 catchment with relative proportions controlled by the precipitations (Smith et al., 2013). However, in this catchment, the
266 mobilization of stream banks has been shown to be effective in winter due to freeze-thaw process (Inamdar et al., under
267 review). This present study analyzed four events sampled in spring and summer. The lower contribution of stream bank
268 erosion could then be due to seasonal variability.

269 The relative proportion of LIG compared to HMW FA plotted against the proportion of α,ω -diacids and ω -hydroxyacids
270 with more than 20 C atoms among HMW FA resulted in a visual differentiation of Li and SBed from W, FH, BaA and BaB
271 and from Up (Figure 5). This observation highlights Li as the main origin of SBed plant-derived OM, which fits well with
272 the high proportion of Li-derived POM in CSS from both catchments. Moreover from Li to SBed, (i) the ratio of coumaric
273 and ferulic acids to vanillaldehyde, acetovanillone and vanillic acid, commonly noted C/V, decreased from 0.79 ± 0.26 to
274 0.20 ± 0.07 , denoted that lignins were more biodegraded in SBed than in Li and (ii) the proportion of microbial markers



275 among the target compounds increased from 12 ± 5 to 48 ± 15 %. Both of these observations highlight the recycling of
276 terrestrial plant-derived OM in river sediments from a headwater catchment, and are in accordance with the higher
277 mineralization rate of soil organic carbon in river sediments (Wang et al., 2014).

278 4.2 Are molecular data in accordance with isotopic and elemental data?

279 A four-step analysis was performed to determine if the molecular data produced by THM-GC-MS were in accordance with
280 the isotopic results (Rowland et al., 2017) previously acquired on those samples.

281 The first one consists in a point-by-point comparison of the source apportionments resulting from the two approaches. Four
282 main observations were reported by Rowland et al. (2017) using the isotopic approach. First, “the litter layer was a dominant
283 contributor to CPOM, especially for the upstream locations”. This is in agreement with our data: the proportion of Li-derived
284 CPOM was 90 ± 11 % and 63 ± 28 % for the 12ha and the 79ha catchments, respectively. Secondly, “the proportional
285 contributions of SBed and banks to MPOM and FPOM increased downstream”. This is also in agreement with molecular
286 data, however stream banks were not considered as a main contributor through the present statistical treatment. The
287 proportion of SBed-derived POM increased from 8 ± 8 % to 49 ± 39 % and from 17 ± 16 % to 38 ± 24 % between the 12 ha
288 and the 79 ha catchments in MPOM and FPOM, respectively. Thirdly, “no appreciable shift was observed in CPOM source”.
289 This is partly in agreement with the molecular data. The main contributor to CPOM was Li in the two locations but the
290 proportion of SBed-derived CPOM increased downstream. Finally, the highest contribution of forest floor humus was
291 observed in MPOM and FPOM for E4. This is in agreement with the source apportionment in this study since the proportion
292 of FH-W-derived POM was the highest for this event in CPOM, MPOM and FPOM from the 12 ha catchment and in MPOM
293 and FPOM from the 79 ha catchment.

294 In a second step, the quality of the source apportionment calculated from the end member mixing approach was investigated
295 by modeling the $\delta^{13}\text{C}$ of the samples using the isotopic fingerprint of end members. These modeled values were compared to
296 the measured values used in the isotopic fingerprinting approach (Rowland et al., 2017). The relative standard deviation was
297 1.1 ± 0.2 % (mean \pm 95% CI; $n = 20$) and the linear regression resulted in a slope of 1.01 ($R^2 = 0.58$; p -value < 0.0001 ;
298 Figure S1) highlighting a fairly good agreement between the model and the data, that is to say between the source
299 apportionment using molecular data and measured $\delta^{13}\text{C}$.

300 In a third step, TOC, $\delta^{13}\text{C}$, $\delta^{15}\text{N}$ and C/N were added as variables in the PCA treatment. In a first PCA, W, FH, Li, SBed,
301 BaA, BaB and Up were considered as potential end members. A HCA using the nine first PCA factors (90.4 % of the
302 variance) highlighted BaA, BaB and Up as minor contributors, similarly to this step performed on molecular data alone.
303 Then a second PCA was calculated with FH, W, Li and SBed as potential end members and the CSS as additional
304 individuals. The two first factors represented 64.4 % of the variance and resulted in a clear differentiation between Li, SBed
305 and FH-W. The same approach was then applied using the molecular data alone, resulting in the calculation of the
306 proportions of those three end members in the CSS for ten different combinations of the position of end members in the 2D



307 plan created by the two first factors of the PCA. For each CSS sample a set of ten values was created for Li-, SBed- and FH-
308 W-derived POM (Table S2). Student T-test was used to compare these distributions between the modality “molecular data”
309 and the modality “molecular + isotopic, elemental data”. A *p*-value was calculated for each sample. They ranged from 0.08
310 to 0.49 (0.25 ± 0.03 ; mean \pm 95% CI), highlighting that there were no significant differences between the two approaches
311 (Table S3).

312 The final step aimed at investigating to what extent the molecular data are representative of bulk POM. The linear regression
313 between the sum of the concentrations of target compounds (expressed in $\mu\text{g/g}$ of dry solid) and the total organic content
314 (expressed in % of dry solid) resulted in a correlation coefficient of 0.94 (*p*-value < 0.0001 ; Figure S2). This correlation
315 between bulk scale and molecular analyses has already been highlighted for sedimentary and dissolved OM (Jeanneau and
316 Faure, 2010; Jeanneau et al., 2014) and emphasizes the suitability of molecular investigations to determine the sources of
317 OM.

318 Once validated by this four-step comparison, what are the insights provided by the molecular approach on the source
319 apportionment of CPOM, MPOM and FPOM along this Piedmont headwater catchment?

320 **4.3 Modification of the source apportionment as a function of rainfall parameters**

321 These present results may be valuable to investigate the relationships between the sources of exported POM and rainfall
322 characteristics. However they have been acquired on only four events and this part of the discussion should be enriched by
323 future investigations.

324 Rainfall is the primary driver for C export since it controls soil erosion and stream discharge (Raymond and Oh, 2007).
325 Rainfall amount and API7 have been shown to control the export of POC from headwater catchments (Dhillon and Inamdar,
326 2013, 2014; Jung et al., 2014). Moreover I_{max} and I_{med} have also been identified as important drivers for soil erosion since
327 they control the rainfall erosivity (Wischmeier, 1959). The four investigated events represented a range of rainfall amounts,
328 I_{max}, I_{med} and API7.

329 Linear regression were performed between the proportions of Li-, SBed- and FH-W-derived POM in CPOM, MPOM and
330 FPOM from both catchments against rainfall amount, I_{max}, I_{med} and API7 (Table 1). With only four investigated events,
331 only relationships characterized by Pearson coefficient higher than 0.8 were considered. *p*-Values were not calculated for
332 those regressions since they would not have had any statistical value. With only four events the highlighted relationships
333 must be handled with care and may be seen as guidelines for future works.

334 In the 12 ha catchment, SBed-derived OM was positively related to I_{max} and API7 and negatively related to I_{med}. The
335 positive relationship with API7 was recorded in C and F fractions, while the positive relationship with I_{max} and the negative
336 relationship with I_{med} were recorded only in the F fraction. In the M fraction, SBed-derived OM was related to the total
337 rainfall. However since this fraction represented $22 \pm 4\%$ (mean \pm SD) of the exported particles, this relationship was not
338 considered as representative. In the 12 ha catchment the export of SBed-derived OM would be favored by rainfall
339 characterized by high I_{max} occurring after a period of dryness (Figure 6a). Moreover the proportion of FH-W-derived OM



340 was positively related to Imed in F fraction. This fraction represented 55 ± 21 % (mean \pm SD) of the exported particles,
341 giving some representativity to this observation. A deeper analysis of the relationship between Imed and the proportion of
342 FH-W-derived OM in the different fractions from the 12 ha catchment highlights a concomitant control of API7 (Figure 6b).
343 For similar Imed (E2 versus E4), the proportion of FH-W-derived OM increased in the three fraction with dry antecedent
344 conditions. The activation of the soil reservoir seems to be controlled by both Imed and API7, which could be interpreted as
345 the necessity of a dry period to replenish a stock of soil OM available for soil erosion and that intensive and regular rainfalls
346 could result in higher soil erosion.

347 In the 79 ha catchment, the proportions of Li and FH-W were negatively related to the rainfall amount and the proportion of
348 SBed was positively related to this variable. These relationships were recorded in the C and M fractions, with the exception
349 of FH-W (only in the C fraction). A deeper analysis of the link between the POM source apportionment and the rainfall
350 amount highlights different threshold values for C, M and F fractions (Figure 6c). In M and F fractions, there was a sharp
351 modification of the source of POM between E4 (40.1 mm) and E2 (43.9 mm). The proportion of FH-W-derived POM
352 decreased from 64 ± 20 % to 0 ± 1 % and from 21 ± 22 % to 1 ± 2 %, in the M and F fractions, respectively. These decreases
353 were concomitant with increases in the proportion of SBed-derived POM from 0 ± 0 % to 43 ± 8 % and from 2 ± 2 % to $48 \pm$
354 9 %, in the M and F fractions, respectively. The source apportionment of FPOM remained unchanged by further increases of
355 the rainfall amount, while for MPOM the source apportionment was clearly modified during E1, which was characterized by
356 the highest rainfall amount (148.9 mm). The proportion of Li-derived POM decreased to 0 ± 1 % and the proportion of
357 SBed-derived POM increased from 58 ± 9 % to 95 ± 7 %. The source apportionment of CPOM drastically changed between
358 E2 and E3 (97.4 mm). The proportion of Li-derived POM decreased from 95 ± 8 % to 47 ± 9 % and the proportion of SBed-
359 derived POM increased from 2 ± 4 % to 53 ± 9 %. This source apportionment remained unchanged between E3 and E1.
360 Since the C fraction was the most important during events 1, 2 and 3, its source apportionment was an important driver of the
361 source of total POM. It was mainly modified between events 2 and 3 with a decrease in the proportion of Li-derived POM
362 and an increase in the proportion of SBed-derived POM. From these observations, the threshold value of 75 mm previously
363 found in this catchment with an increase in the slope of the POC exported in kg/ha as a function of the rainfall amount
364 (Dhillon and Inamdar, 2013) falls in the range from 43.9 mm (E2) to 97.4 mm (E3), where the main modifications of the
365 source of POM exported from the 79 ha catchment were observed. The increase in the proportion of SBed-derived POM
366 accompanied with the increase in the proportion of the C fraction could be the result of the exceeding of a threshold value of
367 the hydrodynamism for sediment remobilization.

368 4.4 Benefits and limitations of this molecular fingerprinting approach

369 The present molecular fingerprinting method has benefits and limitations. Among the benefits, when the analysis is
370 performed on-line, that is to say, when the products of the THM are directly sent to the GC, then the analysis needs low
371 sample mass, in the order of 5 to 10 mg. Then this method is based on the molecular composition of OM, which is perfectly
372 suitable to investigate the fate of POM. Moreover it takes advantage of the differences of chemical composition between



373 living organisms (microorganisms versus plants) and in their different parts (leaves versus roots). As a consequence the
374 recorded modifications can be discussed in term of biogeochemistry of POM.

375 However limitations must be considered. Seasonal variability of the molecular fingerprint could exist especially for quickly
376 reactive reservoir such as litter (Williams et al., 2016). In soils, the turnover of OM takes time (> 50 years; Frank et al.,
377 2012). Consequently their molecular fingerprints may be less sensitive to seasonal variations, with the exception of
378 agricultural soils subject to changes in vegetation cover. This limitation can be easily avoided by sampling the most reactive
379 end-members at different seasons. The second and third limitations come from the method itself. First this is a time-
380 consuming method because each compound must be determined with care in each sample. For an analysis, approximately
381 two hours are mandatory. Finally, because it is not only a value given by an analytical tool, using it asks having an expertise
382 in organic geochemistry.

383 When benefits and limitations are well considered, this molecular fingerprinting approach may be particularly suitable to
384 investigate the sources of POM in combination with other fingerprinting approaches.

385 **5 Conclusion**

386 This study emphasizes the suitability of molecular analysis of POM using THM-GC-MS to investigate the sources of POM
387 in headwater catchments. This analytical technique needs less than 5 mg of freeze-dried matter, which makes it realistic in
388 regard of the amount of suspended sediment exported and simple with only freeze-drying as a preparing step. With
389 approximately hundred of target compounds, the provided chemical fingerprint allows for the differentiation of the main
390 sources of exported POM, specifically between litter, surface soils, and in-channel sediments. The fairly good relationships
391 obtained by comparison with the conclusions gained by the isotopic-elemental investigation provide additional evidence in
392 favor of this organic fingerprinting approach. The present data highlight plant litter as the main source of exported POM with
393 an increasing contribution of stream bed sediments downstream. This latter contribution seems to be controlled by the
394 rainfall amount with a threshold phenomenon already observed for quantitative data. The contribution of soil erosion could
395 be controlled by both the median intensity of rainfall and the amount of rain in the previous 7 days. The investigation of
396 additional events in different catchments will be necessary to determine if those results are generic.

397 **Data availability**

398 Data are available on request from the corresponding author.

399 **Acknowledgements**



400 This study was funded by NSF ESPCoR Grant # IIA 1330238 (NEWRnet) and USDA NIFA Grant # 2015-67020-23585.
401 We would like to thank the Fair Hill Natural Resources Management Area for allowing us to conduct this study in the Fair
402 Hill Nature Preserve. Many thanks to students who assisted with sampling including Erin Johnson, Catherine Winters,
403 Chelsea Krieg, Shawn Del Percio, Margaret Orr and Daniel Warner.

404 References

- 405 Adams, J. L., Tipping, E., Bryant, C. L., Helliwell, R. C., Toberman, H. and Quinton, J.: Aged riverine particulate organic
406 carbon in four UK catchments, *Sci. Total Environ.*, 536, 648–654, doi:10.1016/j.scitotenv.2015.06.141, 2015.
- 407 Armas-Herrera, C. M., Dignac, M.-F., Rumpel, C., Arbelo, C. D. and Chabbi, A.: Management effects on composition and
408 dynamics of cutin and suberin in topsoil under agricultural use, *Eur. J. Soil Sci.*, 67(4), 360–373, doi:10.1111/ejss.12328,
409 2016.
- 410 Challinor, J. M.: Characterisation of wood by pyrolysis derivatisation—gas chromatography/mass spectrometry, *J. Anal.*
411 *Appl. Pyrolysis*, 35(1), 93–107, doi:10.1016/0165-2370(95)00903-R, 1995.
- 412 Collins, A. . and Walling, D. .: Selecting fingerprint properties for discriminating potential suspended sediment sources in
413 river basins, *J. Hydrol.*, 261(1), 218–244, doi:10.1016/S0022-1694(02)00011-2, 2002.
- 414 Derenne, S. and Quénéa, K.: Analytical pyrolysis as a tool to probe soil organic matter, *J. Anal. Appl. Pyrolysis*, 111, 108–
415 120, doi:10.1016/j.jaap.2014.12.001, 2015.
- 416 Dhillon, G. S. and Inamdar, S.: Extreme storms and changes in particulate and dissolved organic carbon in runoff: Entering
417 uncharted waters?, *Geophys. Res. Lett.*, 40(7), 1322–1327, doi:10.1002/grl.50306, 2013.
- 418 Dhillon, G. S. and Inamdar, S.: Storm event patterns of particulate organic carbon (POC) for large storms and differences
419 with dissolved organic carbon (DOC), *Biogeochemistry*, 118(1), 61–81, doi:10.1007/s10533-013-9905-6, 2014.
- 420 Fox, J. F. and Papanicolaou, A. N.: Application of the spatial distribution of nitrogen stable isotopes for sediment tracing at
421 the watershed scale, *J. Hydrol.*, 358(1), 46–55, doi:10.1016/j.jhydrol.2008.05.032, 2008.
- 422 Frank, D. A., Pontes, A. W. and McFarlane, K. J.: Controls on Soil Organic Carbon Stocks and Turnover Among North
423 American Ecosystems, *Ecosystems*, 15(4), 604–615, doi:10.1007/s10021-012-9534-2, 2012.
- 424 Frostegård, Å., Tunlid, A. and Bååth, E.: Phospholipid Fatty Acid Composition, Biomass, and Activity of Microbial
425 Communities from Two Soil Types Experimentally Exposed to Different Heavy Metals, *Appl. Environ. Microbiol.*, 59(11),
426 3605–3617, 1993.
- 427 Galy, V., Peucker-Ehrenbrink, B. and Eglinton, T.: Global carbon export from the terrestrial biosphere controlled by erosion,
428 *Nature*, 521(7551), 204–207, 2015.
- 429 Goñi, M. A., Hatten, J. A., Wheatcroft, R. A. and Borgeld, J. C.: Particulate organic matter export by two contrasting small
430 mountainous rivers from the Pacific Northwest, U.S.A., *J. Geophys. Res. Biogeosciences*, 118(1), 112–134,
431 doi:10.1002/jgrg.20024, 2013.



- 432 Gourdin, E., Huon, S., Evrard, O., Ribolzi, O., Bariac, T., Sengtaheuanghoung, O. and Ayrault, S.: Sources and export of
433 particle-borne organic matter during a monsoon flood in a catchment of northern Laos, *Biogeosciences*, 12(4), 1073–1089,
434 doi:10.5194/bg-12-1073-2015, 2015.
- 435 Huon, S., Evrard, O., Gourdin, E., Lefèvre, I., Bariac, T., Reyss, J.-L., Henry des Tureaux, T., Sengtaheuanghoung, O.,
436 Ayrault, S. and Ribolzi, O.: Suspended sediment source and propagation during monsoon events across nested sub-
437 catchments with contrasted land uses in Laos, *J. Hydrol. Reg. Stud.*, 9, 69–84, doi:10.1016/j.ejrh.2016.11.018, 2017.
- 438 IPCC, 2001. *Climate Change. The IPCC Third Assessment Report. Volumes I (Science), II (Impacts and Adaptation) and III*
439 *(Mitigation Strategies)*. Cambridge Univ Press, Cambridge.
- 440 Jeanneau, L., Jaffrezic, A., Pierson-Wickmann, A.-C., Gruau, G., Lambert, T. and Petitjean, P.: Constraints on the Sources
441 and Production Mechanisms of Dissolved Organic Matter in Soils from Molecular Biomarkers, *Vadose Zone J.*, 13(7),
442 doi:10.2136/vzj2014.02.0015, 2014.
- 443 Jeanneau, L., Denis, M., Pierson-Wickmann, A.-C., Gruau, G., Lambert, T. and Petitjean, P.: Sources of dissolved organic
444 matter during storm and inter-storm conditions in a lowland headwater catchment: constraints from high-frequency
445 molecular data, *Biogeosciences*, 12(14), 4333–4343, doi:10.5194/bg-12-4333-2015, 2015.
- 446 Jeong, J.-J., Bartsch, S., Fleckenstein, J. H., Matzner, E., Tenhunen, J. D., Lee, S. D., Park, S. K. and Park, J.-H.: Differential
447 storm responses of dissolved and particulate organic carbon in a mountainous headwater stream, investigated by high-
448 frequency, in situ optical measurements, *J. Geophys. Res. Biogeosciences*, 117(G3), n/a-n/a, doi:10.1029/2012JG001999,
449 2012.
- 450 Jung, B.-J., Lee, H.-J., Jeong, J.-J., Owen, J., Kim, B., Meusburger, K., Alewell, C., Gebauer, G., Shope, C. and Park, J.-H.:
451 Storm pulses and varying sources of hydrologic carbon export from a mountainous watershed, *J. Hydrol.*, 440, 90–101,
452 doi:10.1016/j.jhydrol.2012.03.030, 2012.
- 453 Jung, B.-J., Lee, J.-K., Kim, H. and Park, J.-H.: Export, biodegradation, and disinfection byproduct formation of dissolved
454 and particulate organic carbon in a forested headwater stream during extreme rainfall events, *Biogeosciences*, 11(21), 6119–
455 6129, doi:10.5194/bg-11-6119-2014, 2014.
- 456 Jung, B.-J., Jeanneau, L., Alewell, C., Kim, B. and Park, J.-H.: Downstream alteration of the composition and
457 biodegradability of particulate organic carbon in a mountainous, mixed land-use watershed, *Biogeochemistry*, 122(1), 79–99,
458 doi:10.1007/s10533-014-0032-9, 2015.
- 459 Koiter, A. J., Lobb, D. A., Owens, P. N., Peticrew, E. L., Tiessen, K. H. D. and Li, S.: Investigating the role of connectivity
460 and scale in assessing the sources of sediment in an agricultural watershed in the Canadian prairies using sediment source
461 fingerprinting, *J. Soils Sediments*, 13(10), 1676–1691, doi:10.1007/s11368-013-0762-7, 2013.
- 462 Kolattukudy, P.: Polyesters in Higher Plants, in *Biopolyesters*, vol. 71, edited by W. Babel and A. Steinbüchel, pp. 1–49,
463 Springer Berlin Heidelberg. [online] Available from: http://dx.doi.org/10.1007/3-540-40021-4_1, 2001.
- 464 Lee, C. S., Sung, T. M., Kim, H. S. and Jeon, C. H.: Classification of forensic soil evidences by application of THM-
465 PyGC/MS and multivariate analysis, *J. Anal. Appl. Pyrolysis*, 96, 33–42, doi:10.1016/j.jaap.2012.02.017, 2012.



- 466 Ludwig, W., Probst, J.-L. and Kempe, S.: Predicting the oceanic input of organic carbon by continental erosion, *Glob.*
467 *Biogeochem. Cycles*, 10(1), 23–41, doi:10.1029/95GB02925, 1996.
- 468 Mannino, A. and Harvey, H. R.: Terrigenous dissolved organic matter along an estuarine gradient and its flux to the coastal
469 ocean, *Org. Geochem.*, 31(12), 1611–1625, doi:10.1016/S0146-6380(00)00099-1, 2000.
- 470 Mueller, K. E., Polissar, P. J., Oleksyn, J. and Freeman, K. H.: Differentiating temperate tree species and their organs using
471 lipid biomarkers in leaves, roots and soil, *Org. Geochem.*, 52, 130–141, doi:10.1016/j.orggeochem.2012.08.014, 2012.
- 472 Nierop, K. G. J. and Verstraten, J. M.: Rapid molecular assessment of the bioturbation extent in sandy soil horizons under
473 pine using ester-bound lipids by on-line thermally assisted hydrolysis and methylation-gas chromatography/mass
474 spectrometry, *Rapid Commun. Mass Spectrom.*, 18(10), 1081–1088, doi:10.1002/rcm.1449, 2004.
- 475 Nierop, K. G. J., Preston, C. M. and Kaal, J.: Thermally Assisted Hydrolysis and Methylation of Purified Tannins from
476 Plants, *Anal. Chem.*, 77(17), 5604–5614, doi:10.1021/ac050564r, 2005.
- 477 Nosrati, K., Govers, G., Ahmadi, H., Sharifi, F., Amoozegar, M. A., Merckx, R. and VanMaerke, M.: An exploratory study
478 on the use of enzyme activities as sediment tracers: biochemical fingerprints?, *Int. J. Sediment Res.*, 26(2), 136–151,
479 doi:10.1016/S1001-6279(11)60082-6, 2011.
- 480 Oeurng, C., Sauvage, S., Coynel, A., Maneux, E., Etcheber, H. and Sánchez-Pérez, J.-M.: Fluvial transport of suspended
481 sediment and organic carbon during flood events in a large agricultural catchment in southwest France, *Hydrol. Process.*,
482 25(15), 2365–2378, doi:10.1002/hyp.7999, 2011.
- 483 Raymond, P. A. and Oh, N.-H.: An empirical study of climatic controls on riverine C export from three major U.S.
484 watersheds, *Glob. Biogeochem. Cycles*, 21(2), n/a-n/a, doi:10.1029/2006GB002783, 2007.
- 485 Ritchie, J. C., Spraberry, J. A. and McHenry, J. R.: Estimating Soil Erosion from the Redistribution of Fallout ¹³⁷Cs₁, *Soil*
486 *Sci. Soc. Am. J.*, 38(1), 137–139, doi:10.2136/sssaj1974.03615995003800010042x, 1974.
- 487 Rowland, R., Inamdar, S. and Parr, T.: Evolution of particulate organic matter (POM) along a headwater drainage: role of
488 sources, particle size class, and storm magnitude, *Biogeochemistry*, 133(2), 181–200, doi:10.1007/s10533-017-0325-x, 2017.
- 489 Smith, J. C., Galy, A., Hovius, N., Tye, A. M., Turowski, J. M. and Schleppl, P.: Runoff-driven export of particulate organic
490 carbon from soil in temperate forested uplands, *Earth Planet. Sci. Lett.*, 365, 198–208, doi:10.1016/j.epsl.2013.01.027, 2013.
- 491 Tamoooh, F., Van den Meersche, K., Meysman, F., Marwick, T. R., Borges, A. V., Merckx, R., Dehairs, F., Schmidt, S.,
492 Nyunja, J. and Bouillon, S.: Distribution and origin of suspended matter and organic carbon pools in the Tana River Basin,
493 Kenya, *Biogeosciences*, 9(8), 2905–2920, doi:10.5194/bg-9-2905-2012, 2012.
- 494 Tank, J. L., Rosi-Marshall, E. J., Griffiths, N. A., Entekin, S. A. and Stephen, M. L.: A review of allochthonous organic
495 matter dynamics and metabolism in streams, *J. North Am. Benthol. Soc.*, 29(1), 118–146, doi:10.1899/08-170.1, 2010.
- 496 Wallbrink, P. J. and Murray, A. S.: Distribution and Variability of ⁷Be in Soils Under Different Surface Cover Conditions
497 and its Potential for Describing Soil Redistribution Processes, *Water Resour. Res.*, 32(2), 467–476,
498 doi:10.1029/95WR02973, 1996.



- 499 Walling, D. E.: Use of ^{137}Cs and other fallout radionuclides in soil erosion investigations: progress, problems and prospects,
500 Joint FAO/IAEA Division of Nuclear Techniques in Food and Agriculture, International Atomic Energy Agency (IAEA),
501 Vienna (Austria). [online] Available from:
502 http://www.iaea.org/inis/collection/NCLCollectionStore/_Public/29/049/29049354.pdf, 1998.
- 503 Walling, D. E.: The evolution of sediment source fingerprinting investigations in fluvial systems, *J. Soils Sediments*, 13(10),
504 1658–1675, doi:10.1007/s11368-013-0767-2, 2013.
- 505 Wang, X., Cammeraat, E. L. H., Romeijn, P. and Kalbitz, K.: Soil Organic Carbon Redistribution by Water Erosion – The
506 Role of CO_2 Emissions for the Carbon Budget, *PLOS ONE*, 9(5), e96299, doi:10.1371/journal.pone.0096299, 2014.
- 507 Williams, J. S., Dungait, J. A. J., Bol, R. and Abbott, G. D.: Contrasting temperature responses of dissolved organic carbon
508 and phenols leached from soils, *Plant Soil*, 399, 13–27, doi:10.1007/s11104-015-2678-z, 2016.
- 509 Wischmeier, W. H.: A Rainfall Erosion Index for a Universal Soil-Loss Equation1, *Soil Sci. Soc. Am. J.*, 23(3), 246–249,
510 doi:10.2136/sssaj1959.03615995002300030027x, 1959.

511 **Figure captions**

- 512 Figure 1: Location of the study watershed in the Piedmont region of Maryland. Composite suspended sediments were
513 sampled at the 12 and 79 ha locations (grey circles). The sites of collection of end-members are indicated with triangles:
514 violet for Wet, blue for Bsed, green for FH and Li, orange for Up and yellow for BaA and BaB.
- 515 Figure 2: Relative proportions of low organic acids (LOA), phenolic compounds (PHE), low molecular weight and high
516 molecular weight fatty acids (LMW and HMW FA) and carbohydrates (CAR) among identified target compounds in the end
517 members. Uncertainties correspond to standard deviation of sampling triplicates (duplicates for Sbed).
- 518 Figure 3: Relative proportions of low organic acids (LOA), phenolic compounds (PHE), low molecular weight and high
519 molecular weight fatty acids (LMW and HMW FA) and carbohydrates (CAR) among identified target compounds in the
520 coarse, medium and fine fractions of CSS. Uncertainties correspond to the inter-event standard deviation.
- 521 Figure 4: Plan defined by the two first factors of the PCA calculated using the distribution of target compounds. Squares
522 represent end members Li (green), FH-W (red) and Sbed (blue). The area characteristic of each end member is defined by the
523 95% confident interval. Circles represent CSS from the 12 ha (orange) and the 79 ha (purple) locations. The mean positions
524 for each size fraction are represented by large circles and uncertainties correspond to inter-event standard deviation.
- 525 Figure 5: 2D plot illustrating the variability of the distribution of plant-derived markers using the relative proportion of PHE
526 against HMW FA and the proportion of a,w diacids and wOH fatty acids among HMW FA (denoted HMW FA ratio).
- 527 Figure 6: Illustration of the most significant correlations between the source apportionments performed using the molecular
528 data and rainfall characteristics. At the 12 ha location, positive correlations (a) between the proportion of Sbed-derived POM
529 and I_{max} and (b) between the proportion of FH-W-derived POM and I_{med} . At the 79 ha location, positive correlation



530 between Sbed-derived POM and rainfall amount (c). Coarse, medium and fine fractions are depicted by the dark grey, light
531 grey and white circles, respectively and the composite POM by the black diamond.



Table 1. Rainfall characteristics, discharge and proportion of coarse, medium and fine fractions for the 4 investigated storm events.

| | Event 1 | | Event 2 | | Event 3 | | Event 4 | |
|------------------------------------|--------------------|--------------|----------------------|--------------|---------------------|--------------|-----------------------|--------------|
| | <i>May 1, 2014</i> | | <i>Apr. 21, 2015</i> | | <i>July 3, 2015</i> | | <i>Sept. 30, 2015</i> | |
| Rainfall | | | | | | | | |
| total (mm) | 148.9 | | 43.9 | | 97.4 | | 40.1 | |
| max (mm h ⁻¹) | 19.9 | | 20 | | 31.3 | | 20.2 | |
| median (mm h ⁻¹) | 1.3 | | 2.2 | | 0.4 | | 2.1 | |
| API7 (mm) | 9.7 | | 10.4 | | 68.2 | | 0 | |
| Discharge (12 ha catchment) | | | | | | | | |
| max (l s ⁻¹) | 150.1 | | 68.3 | | 87.4 | | 15.5 | |
| Particle size distribution | | | | | | | | |
| | <i>12 ha</i> | <i>79 ha</i> | <i>12 ha</i> | <i>79 ha</i> | <i>12 ha</i> | <i>79 ha</i> | <i>12 ha</i> | <i>79 ha</i> |
| Coarse (%) | 52 | 81 | 20 | 43 | 12 | 58 | 6 | nd |
| Medium (%) | 22 | 13 | 22 | 32 | 27 | 20 | 18 | nd |
| Fine (%) | 27 | 7 | 59 | 25 | 61 | 21 | 75 | nd |

532

533



Table 2. Source apportionment calculated using the molecular data.

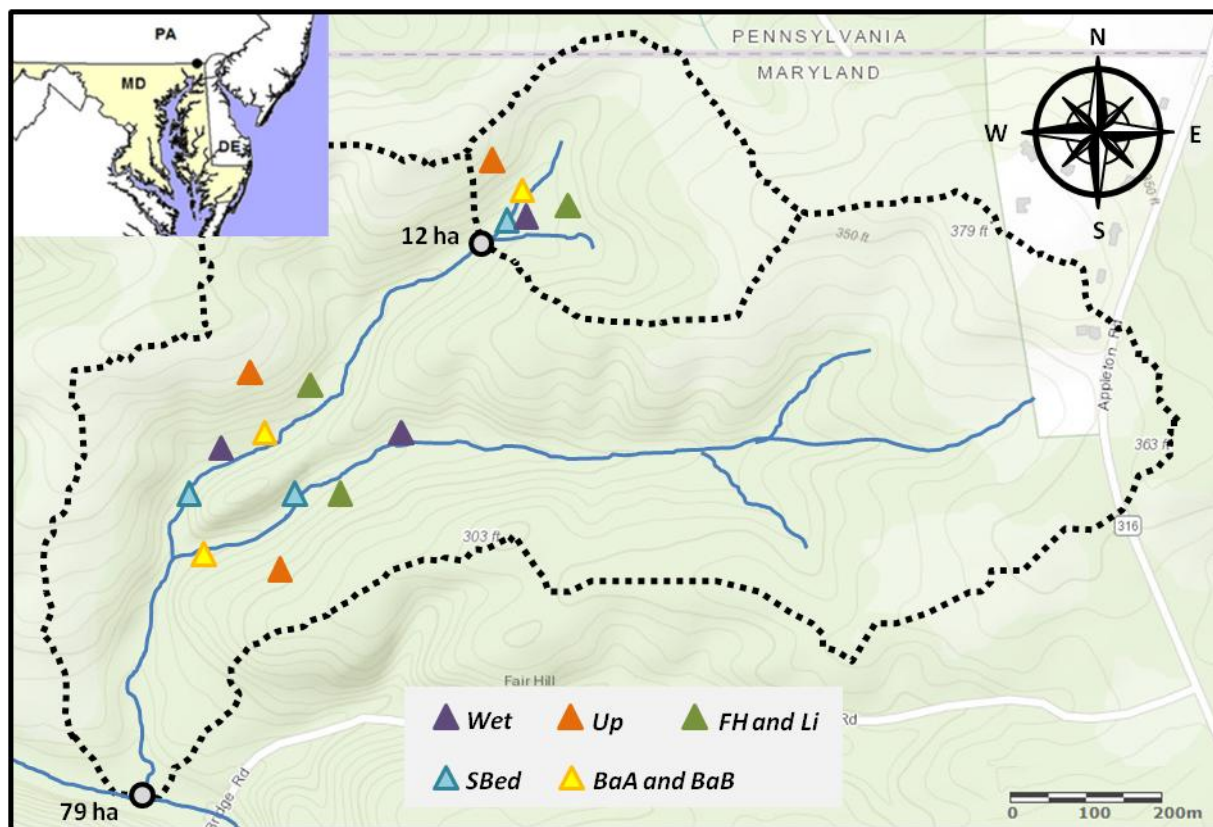
| | | <i>12 ha location</i> | | | <i>79 ha location</i> | | |
|---|-----|-----------------------|----------|----------|------------------------|----------|----------|
| | | Li (%) | Sbed (%) | FH-W (%) | Li (%) | Sbed (%) | FH-W (%) |
| Event 1 <i>May 1, 2014</i> | C | 97 ± 7 | 1 ± 2 | 3 ± 7 | 45 ± 9 | 55 ± 9 | 0 ± 0 |
| | M | 78 ± 7 | 18 ± 5 | 4 ± 8 | 0 ± 1 | 95 ± 7 | 4 ± 7 |
| | F | 76 ± 12 | 13 ± 6 | 11 ± 16 | 48 ± 9 | 52 ± 9 | 0 ± 0 |
| | POM | 92 ± 9 | 4 ± 4 | 4 ± 11 | 42 ± 6 | 57 ± 8 | 0 ± 2 |
| Event 2 <i>Apr. 21, 2015</i> | C | 95 ± 8 | 2 ± 3 | 3 ± 8 | 95 ± 8 | 2 ± 4 | 3 ± 8 |
| | M | 94 ± 9 | 2 ± 3 | 4 ± 9 | 57 ± 9 | 43 ± 8 | 0 ± 1 |
| | F | 69 ± 16 | 15 ± 6 | 17 ± 20 | 51 ± 10 | 48 ± 9 | 1 ± 2 |
| | POM | 86 ± 11 | 6 ± 4 | 8 ± 12 | 89 ± 9 | 8 ± 7 | 3 ± 4 |
| Event 3 <i>July 3, 2015</i> | C | 96 ± 5 | 3 ± 4 | 1 ± 5 | 47 ± 9 | 53 ± 9 | 0 ± 0 |
| | M | 87 ± 6 | 10 ± 5 | 3 ± 7 | 42 ± 9 | 58 ± 9 | 0 ± 0 |
| | F | 61 ± 8 | 39 ± 7 | 0 ± 1 | 45 ± 11 | 51 ± 9 | 4 ± 6 |
| | POM | 81 ± 6 | 17 ± 6 | 2 ± 4 | 46 ± 10 | 53 ± 9 | 2 ± 2 |
| Event 4 <i>Sept. 30, 2015</i> | C | 73 ± 22 | 0 ± 0 | 27 ± 22 | fraction not available | | |
| | M | 70 ± 22 | 0 ± 0 | 30 ± 22 | 36 ± 20 | 0 ± 0 | 64 ± 22 |
| | F | 62 ± 23 | 0 ± 0 | 38 ± 23 | 77 ± 20 | 2 ± 2 | 21 ± 22 |
| | POM | 65 ± 23 | 0 ± 0 | 35 ± 23 | - | - | - |

534

535



536 **Figure 01**

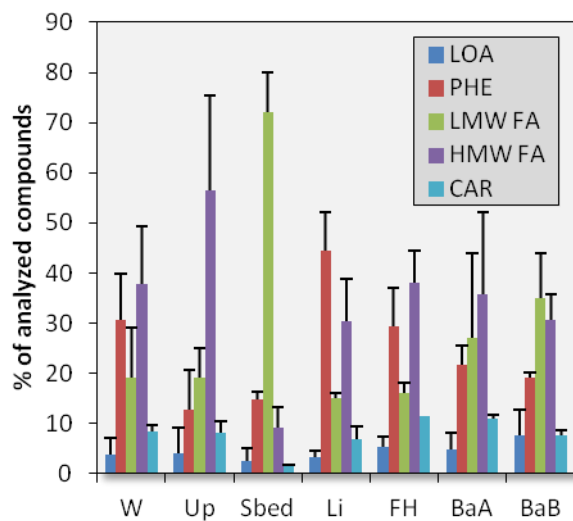


537

538



539 **Figure 02**

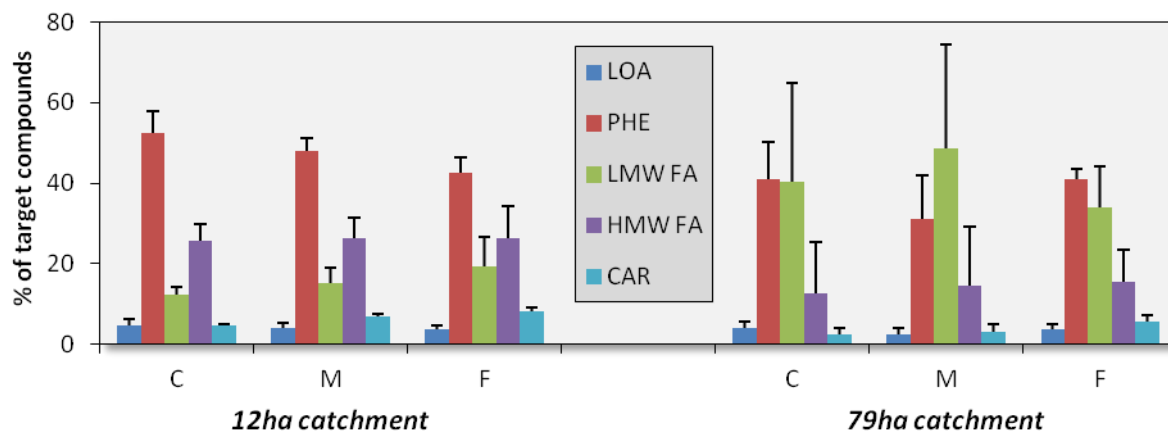


540

541



542 **Figure 03**

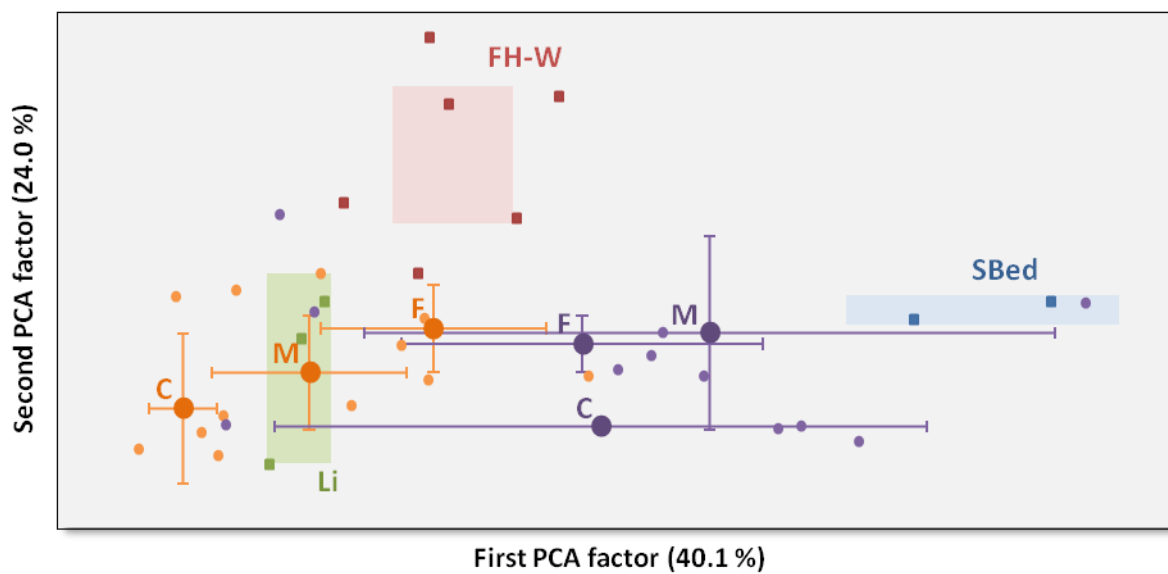


543

544



545 **Figure 04**

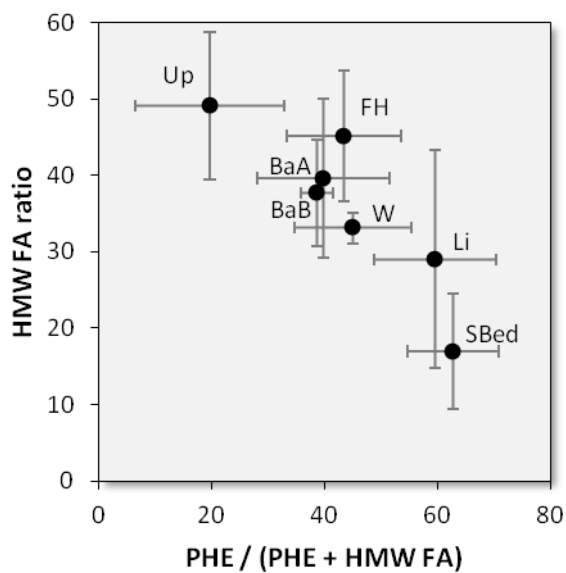


546

547



548 **Figure 05**

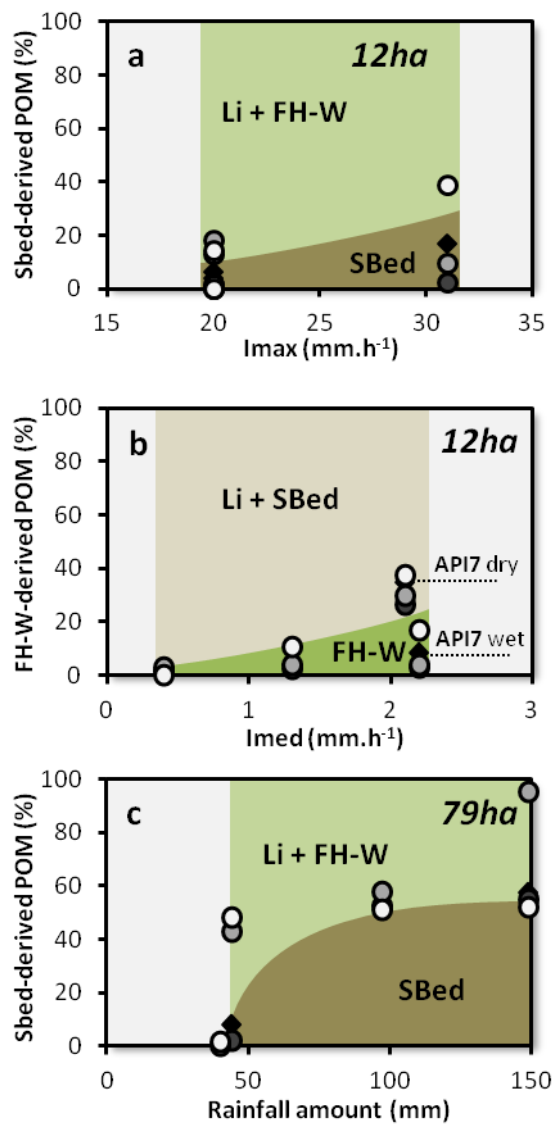


549

550



551 **Figure 06**



552

553

554